International Research Journal of Engineering and Technology (IRJET) e-ISSN: 2395-0056
Volume: 08 Issue: 06 | June 2021 www.irjet.net p-ISSN: 2395-0072

Brain SCAT – Segmentation and Classification of Brain Tumor

Arsya Mohamed Ali[1], Melvin Martin[2], Nithin Gangadharan Rangaraj[3]

[1,2,3]*Student, Dept. of Biomedical Engineering, PSG College of Technology, Tamil Nadu, India*

Abstract – *Diagnosis of brain tumor helps in anticipating the severity of its impact which would help the medical personnel in treating the patients efficiently thereby increasing their survival rate. Localizing the tumor and identifying its type are the preliminary steps in brain tumor diagnosis that involve specialized clinicians. Computer vision automates these tasks in a time-conservative manner. Brain SCAT, a user-accessible platform is developed incorporating a deep learning model that performs segmentation and classification jointly.*

Key Words: Classification, Segmentation, Brain tumor, Computer vision, Dashboard, U-Net.

1. INTRODUCTION

Brain tumors refer to the unnecessary growth of cells within the brain. The presence of tumors in the primary organ, the brain, often causes fatal issues to the patients thereby increasing the mortality rate. Brain tumors are classified into two types, namely, benign, and malignant tumors. According to the International Association of Cancer Registries (IARC), in India, approximately 28,000 patients are diagnosed with brain tumors annually. Furthermore, these tumors cause the death of around 24,000 patients every year [1].

Computer Vision assists healthcare professionals in diagnosing and monitoring diseases thereby prescribing the right treatment. The application of this technology eliminates a lot of time spent on traditional diagnostic procedures and hence, medical professionals would be able to concentrate better on patients. These techniques extend the efficiency of treatment as they are not limited to human perception alone which is subjected to medical negligence.

A hybrid model is developed to perform both segmentation and classification of tumors jointly. This model incorporates a conventional U-Net architecture developed by Olaf Ronneberger et al [2] for executing the segmentation task. After suitable evaluation, the trained model is then deployed using Heroku and Dash.

2. DATASET

The dataset contains MRI images collected from Nanfang and General hospital, Tianjing Medical University, China from 2005 to 2010 [3]. This dataset hosts 3064 T1-weighted MRI images of 233 patients diagnosed with three types of tumors, namely, meningioma, glioma, and pituitary tumor. The distribution of the three classes is shown in figure 1.

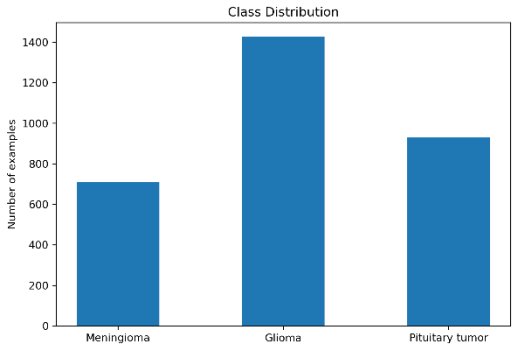

Fig -1: Distribution of classes

Meningioma is a type of non-cancerous tumor that arises from the meninges, the membrane surrounding the brain and spinal cord. Glioma refers to a tumor that originates from the glial cells of the brain, brain stem, or spinal column. The glial cells are those that support the other brain cells, the neurons. The abnormal non-cancerous growth in the pituitary gland is called a pituitary tumor.

The images and metadata exist together as a matlab data format in the dataset. The images are of 512 x 512-pixel size. The masks are binary images where 1's indicate the region of the tumor. The sample images and the respective masks are shown in figure 2. In addition, the classes are encoded as 1,2, and 3 for meningioma, glioma, and pituitary tumor respectively.

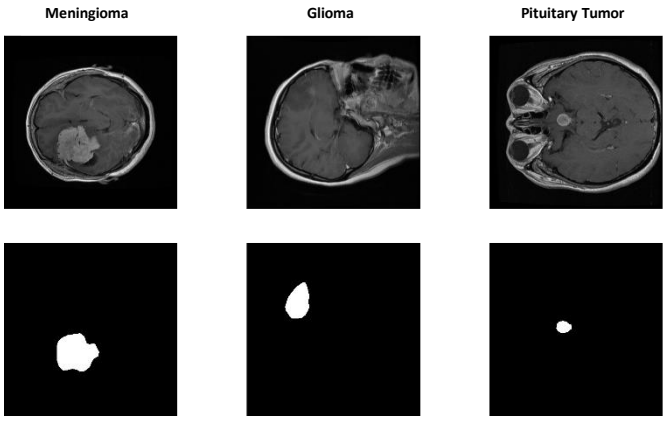

Fig -2: Sample images with masks

3. DATA PREPROCESSING

The dataset mentioned in section 2 is transformed into an efficient format by implementing few preprocessing techniques. Each .mat file has image data and its metadata of which only the label, image data, and tumor mask are extracted. The image data and the tumor mask are then converted into a NumPy array. The uint16 NumPy array of the image is mapped to the uint8 NumPy array and the tumor mask is transformed to binary data from Boolean. The resultant NumPy array of the images and the masks are saved as images using the pillow library as separate folders.

The train-val-test split ratio of the dataset is 75:22:3 where 2299 images are used for training, 700 images for validating, and 64 images for testing the model. To overcome class imbalance and to prevent overfitting, image augmentation is performed on the training dataset and the sample augmented images can be seen in figure 3. The augmentation operations are shown in table 1.

Operations	Value
Rescaling	255
Zoom	0.3
Shear Range	0.2

Table -1: Augmentation Parameters

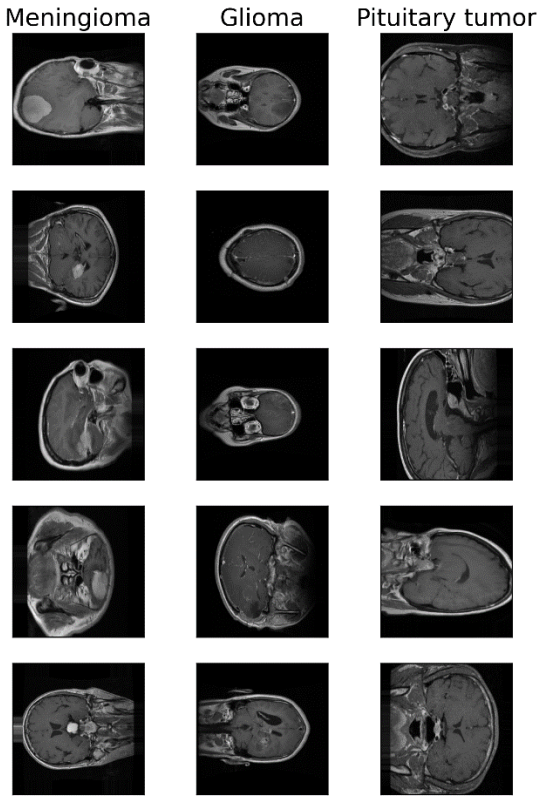

Fig -3: Augmented Sample X-Ray Image

4. MODEL ARCHITECTURE

An overall model architecture is developed for both segmentation and classification of brain tumors which is shown in figure 4. The input is fed into two blocks namely, the U-net and the custom CNN which are used for segmentation and classification respectively.

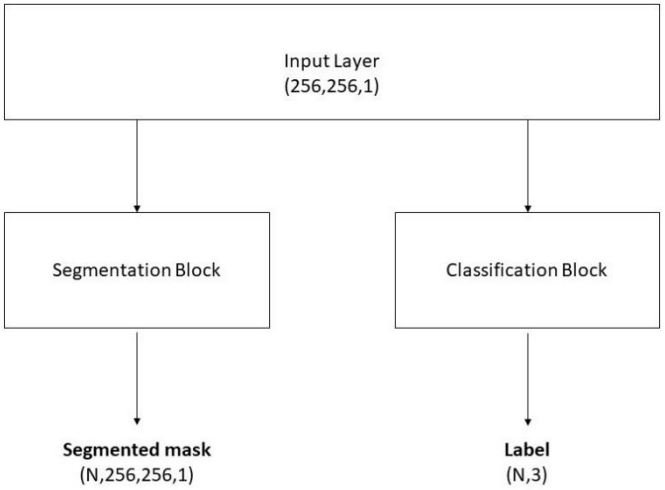

Fig -4: Block Diagram of Model Architecture

The block that performs tumor segmentation employs a U-net architecture which is a conventional neural network mainly used for segmenting biomedical images. Its architecture consists of an encoder network followed by a decoder network. The convolutional layers are activated by the ReLU function and the sigmoid operation is used in the output layer. The U-net architecture is shown below in figure 5.

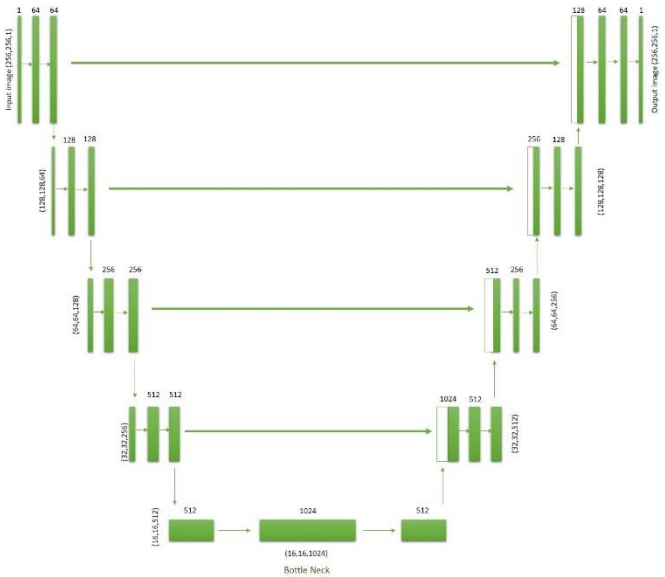

Fig -5: U-Net Architecture

A custom CNN block consisting of convolutional, max pooling, flatten, and dense layers is developed for classifying the type of brain tumor which is shown in figure 6. ReLU operation is used in convolutional layers and to obtain the class, SoftMax activation function is employed in the output layer which turns logits into probabilities.

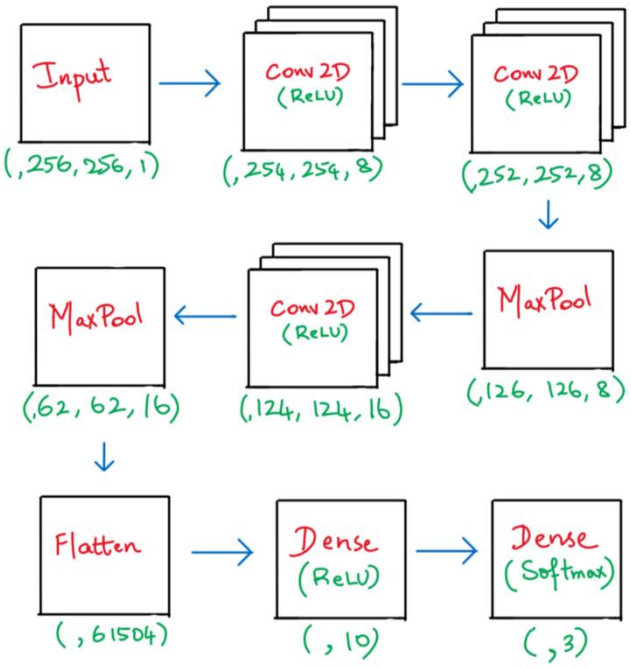

Fig -6: Custom CNN Architecture

5. MODEL TRAINING AND EVALUATION

The model is architected in such a way that it has a single input and two outputs for segmentation and classification purposes as mentioned in section 4. As a result, multiple loss functions are defined. The summation of binary cross-entropy and dice loss is known as BCE-Dice loss is used as a loss function for segmentation. BCE calculates the probabilities by penalizing the logits based on the distance from the expected value. The BCE formula is shown in equation 1.

$$BCE = -\frac{1}{N}\sum_{i=0}^{N} y_i \cdot log(\hat{y}_i) + (1 - y_i) \cdot log(1 - \hat{y}_i) \quad (1)$$

The dice coefficient which is shown in equation 2 is a measure of overlap between two samples. It ranges from 0 to 1, where the value 1 depicts that the samples are perfectly.

$$Dice\ Coefficient = \frac{2 * |X \cap Y|}{|X| + |Y|} \quad (2)$$

The classification block uses Categorical Cross-Entropy(CCE) as its loss function. The mathematical equation of CCE is shown in equation 3.

$$CCE = \sum_{i=1}^{\text{output size}} y_i \cdot \log \hat{y}_i \quad (3)$$

The model is trained for a total of 140 epochs using Adam optimizer. Initially, both the segmentation and classification blocks are trained for 30 epochs. Adjusting the loss weights, the segmentation block is trained for another 110 epochs by freezing the weights of classification block layers.

The segmentation block is evaluated based on the IOU score and F1-Score. The Intersection Over Union score quantifies how exactly the target and the predicted images overlap. Accuracy is used to validate the classification block. The evaluation results for each block are shown in table 2.

Metrics	Train	Validation	Test
Segmentation IOU Score	0.71	0.61	0.61
Segmentation F1-Score	0.83	0.74	0.75
Classification Accuracy	0.93	0.88	0.84

Table -2: Performance Metrics

The training curves for the losses and other metrics are shown in figures 7 to 11.

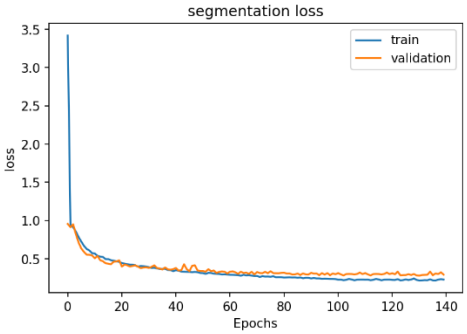

Fig -7: Segmentation Loss

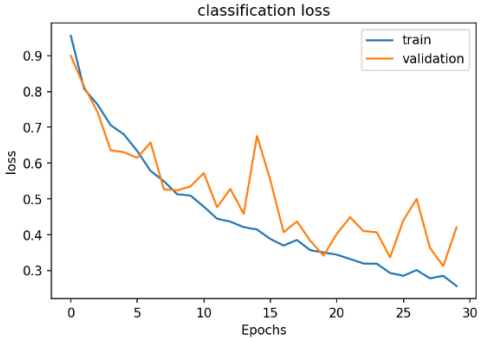

Fig -8: Classification Loss

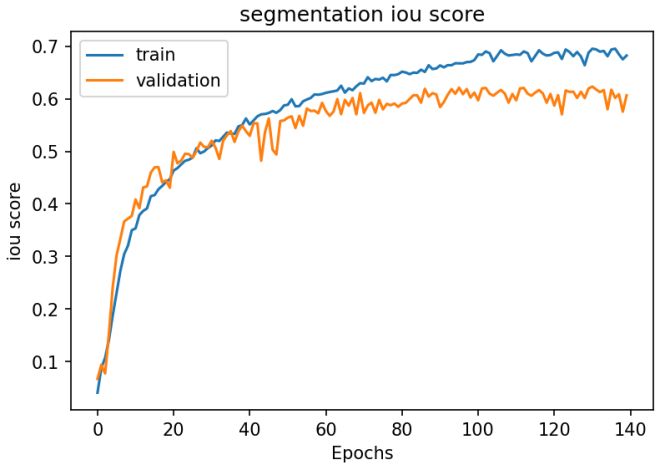

Fig -9: Segmentation IOU Score

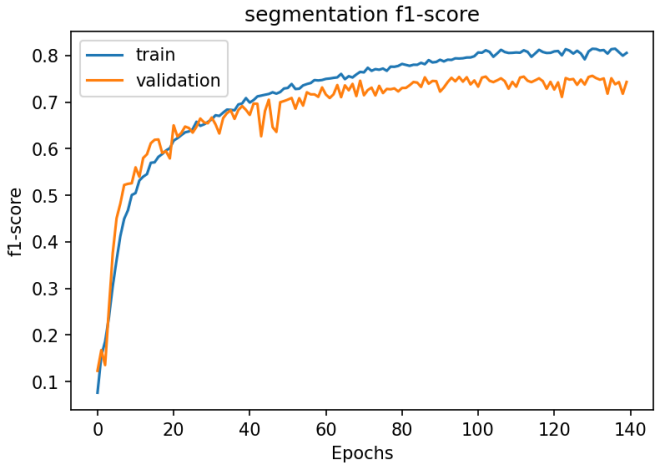

Fig -10: Segmentation F1-Score

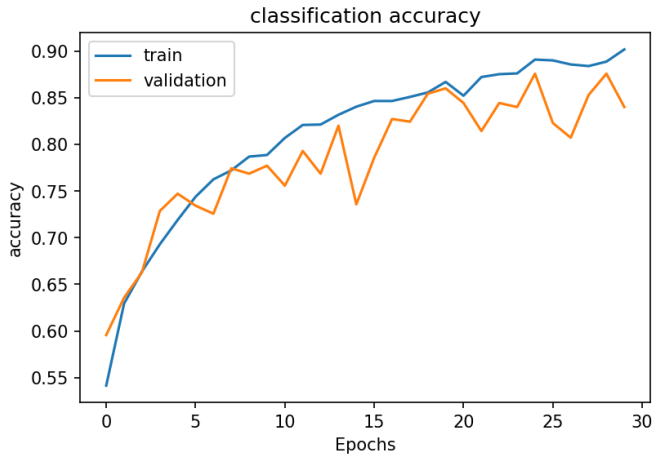

Fig -11: Classification Accuracy

6. RESULTS

The essence of the fully trained model can be realized when the predictions are visualized in real-time. From this perspective, three test images belonging to different classes are provided as inputs and the predicted masks are superimposed with the images to highlight the region of interest as shown in figure 12. The confusion matrix for the classification block can be seen in figure 13.

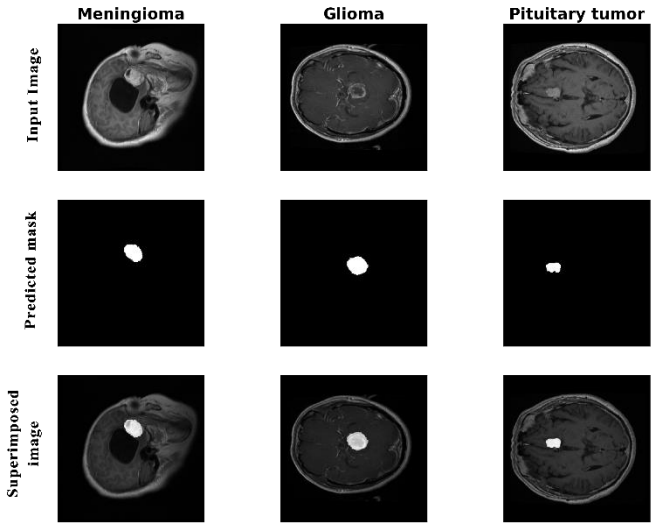

Fig -12: Segmenting test data – Sample Predictions

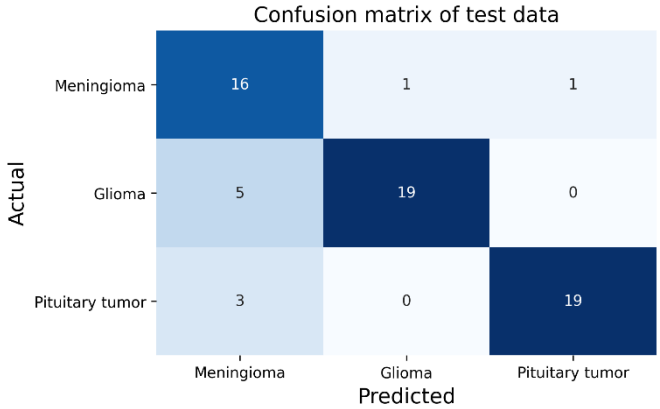

Fig -13: Confusion Matrix of Test Data

In order to derive clinically significant decisions and insights, it is important to seamlessly deploy the model into production. Dash Plotly, a python framework for dashboard development is used to design the front-end application. For model deployment, the trained model of size 140MB is quantized and converted into tflite model of size 70MB. The tflite model along with the associated files are pushed to a GitHub repository which is then bundled and deployed in Heroku. The overall flow is illustrated in figure 14. The screenshots of the front page, result page, and the

generated report are shown in figures 15, 16 & 17 respectively.

Website Link: https://brain-tumor-seg.herokuapp.com

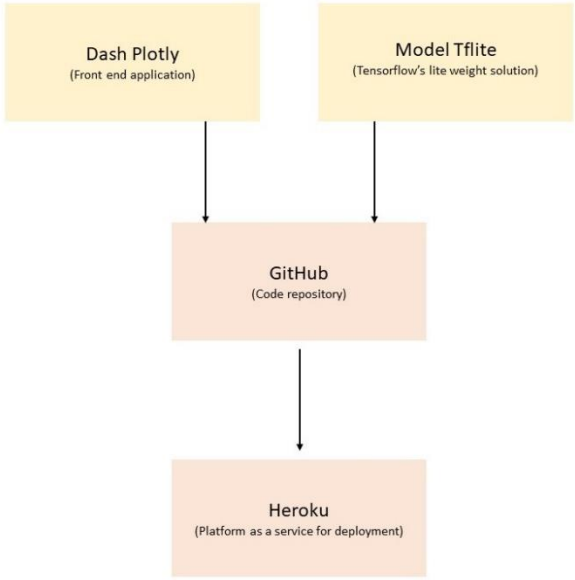

Fig -14: Model Deployment Flow Chart

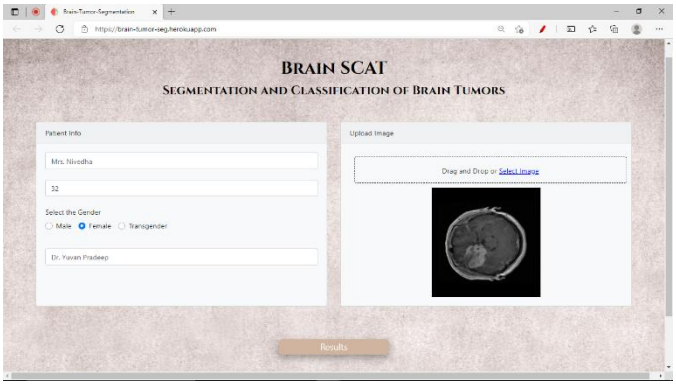

Fig -15: Front Page

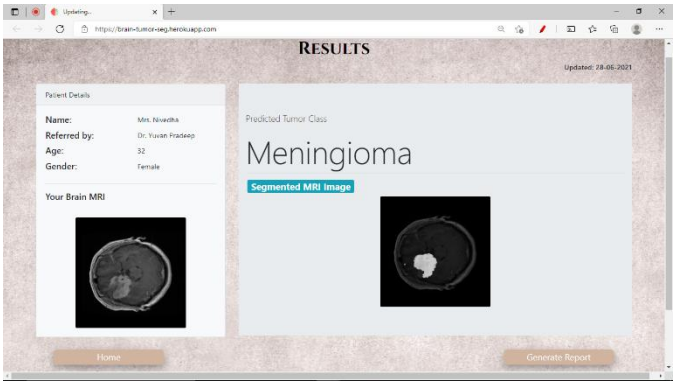

Fig -16: Result Page

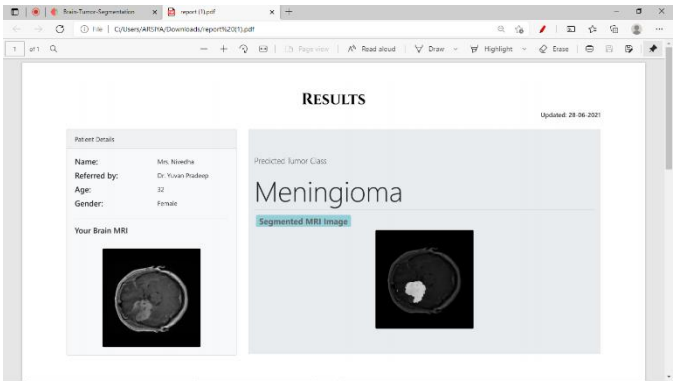

Fig -17: Generated Report

7. CONCLUSIONS

Brain SCAT, an accessible platform to locate and diagnose the type of brain tumor is developed which could ease the overall process of diagnosis for clinicians, thereby achieving the objective. The performance of the model could be further improved by training on a large dataset.

REFERENCES

[1] https://www.narayanahealth.org/brain-tumour/, Accessed on June 2021

[2] Ronneberger O., Fischer P., Brox T. (2015) U-Net: Convolutional Networks for Biomedical Image Segmentation. In: Navab N., Hornegger J., Wells W., Frangi A. (eds) Medical Image Computing and Computer-Assisted Intervention – MICCAI 2015. MICCAI 2015. Lecture Notes in Computer Science, vol 9351. Springer, Cham. https://doi.org/10.1007/978-3-319-24574-4_28

[3] Cheng, Jun (2017): brain tumor dataset. figshare. Dataset.https://doi.org/10.6084/m9.figshare.1512427.v5, Accessed on May 2021